STUDY OF THREE-NUCLEON DYNAMICS IN THE dp BREAKUP COLLISIONS USING THE WASA DETECTOR*

B. Kłos[a], I. Ciepał[b], B. Jamróz[a], G. Khatri[c], S. Kistryn[c]
A. Kozela[b], A. Magiera[c], W. Parol[b], I. Skwira-Chalot[d]
E. Stephan[a]

[a]Institute of Physics, University of Silesia, Chorzów, Poland
[b]H. Niewodniczański Institute of Nuclear Physics, Polish Academy of Sciences
Kraków, Poland
[c]M. Smoluchowski Institute of Physics, Jagiellonian University
Kraków, Poland
[d]Faculty of Physics, University of Warsaw, Warszawa, Poland

(Received December 28, 2017)

An experiment to investigate the $^1\mathrm{H}(d,pp)n$ breakup reaction using a deuteron beam of 300, 340, 380 and 400 MeV and the WASA detector has been performed at the Cooler Synchrotron COSY-Jülich. As a first step, the data collected at the beam energy of 340 MeV are analysed, with a focus on the proton–proton coincidences registered in the Forward Detector. Elastically scattered deuterons are used for precise determination of the luminosity. The main steps of the analysis, including energy calibration, particle identification (PID) and efficiency studies, and their impact on the final accuracy of the result, are discussed.

DOI:10.5506/APhysPolBSupp.11.57

1. Introduction

Few nucleon systems are ideal laboratories to study details of nuclear interactions. Their theoretical and experimental investigation started from the simple nucleon–nucleon ($2N$) systems and gradually evolved into more complex environments. At present, the breakup observables can be calculated using modern realistic pairwise nucleon–nucleon NN interactions, combined with model of $3N$ forces [1]. Moreover, the two- and three-nucleon interactions can be modelled within the coupled-channel (CC) framework by an explicit treatment of the Δ-isobar [2]. Alternatively, the dynamics is generated by the chiral effective field theory (χEFT), so far at the

* Presented at the XXIV Nuclear Physics Workshop "Marie and Pierre Curie", Kazimierz Dolny, Poland, September 20–24, 2017.

next-to-next-to-leading order with all relevant NN and $3N$ contributions taken into account [3]. The new, improved version of ChPT is currently being developed [4]. The modern theoretical calculations include also the long-range Coulomb interaction [5], particularly important at low relative momentum of outgoing protons. Recent years brought important progress in the theoretical calculations with respect to the relativistic treatment of the $3N$ systems. The first predictions were developed using $2N$ potential in [6] and this approach has also been extended for calculations including $3N$F in [7]. The relativistic effects reveal at different parts of the phase-space with various magnitude. It was shown that in some particular regions of the breakup phase space, relativistic effects can increase or decrease the calculated breakup cross sections by up to 60%. With the lack of complete calculations performed in relativistic regime, including $3N$F and Coulomb interaction, there is a need of the systematic (in the beam energy) data set collected in a large phase space. This may allow us to trace the effects in the kinematic regions where they play locally very important role. A new measurement of the ^{1}H$(d,pp)n$ breakup cross section using a deuteron beam of 300, 340, 380 and 400 MeV with the aim to check the theoretical predictions for relativistic effects and to unambiguously fix a relevance of the $3N$F.

2. Experiment

The experiment studying the ^{1}H$(d,pp)n$ breakup reaction at 300 MeV, 340 MeV, 380 MeV and 400 MeV deuteron beam energies has been performed at the Cooler Synchrotron COSY-Jülich with the WASA-at-COSY detector [8,9]. The WASA (Wide Angle Shower Apparatus) detector, covering almost full solid angle, consists of four main components: Central Detector (CD), Forward Detector (FD), Pellet Target Device and Scattering Chamber (see Fig. 1). The acceptance of WASA detection system is close to 4π what

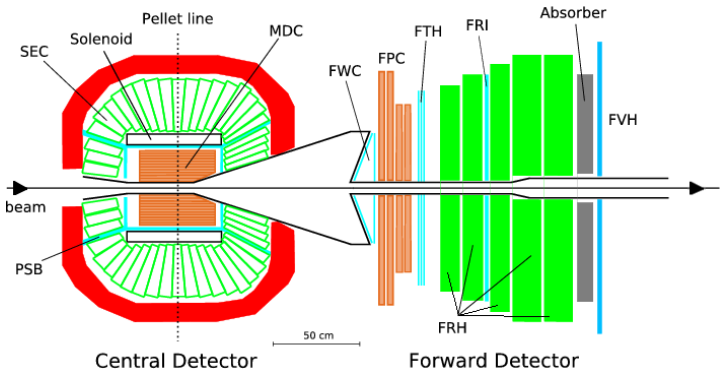

Fig. 1. Schematic view of the detection system.

makes this devices very well suited for measurements of observables for the breakup and elastic scattering reactions, and then gives unique possibility to study various aspects of dynamics in a wide range of kinematic variables.

3. Data analysis

The data analysis is focused on the proton–proton coincidences from the ^{1}H$(d,pp)n$ breakup reaction at 340 MeV deuteron beam energy registered in the Forward Detector. The aim of our study is the determination of the differential cross section on a dense angular grid of kinematical configurations defined by the emission angles of the two outgoing protons: two polar angles θ_1 and θ_2 (in the range between 5° and 15°) and the relative azimuthal angle φ_{12} (in the full range between 20° and 180°).

The first step of data analysis is the identification of interesting events, *i.e.* two protons from the breakup process and deuterons from the elastic scattering channel in the Forward Detector (range of the polar angles is from 3° to 18°). The particle identification is based on the ΔE–E technique. In the whole range of energies, a clear separation between loci of protons and deuterons is observed (Fig. 2).

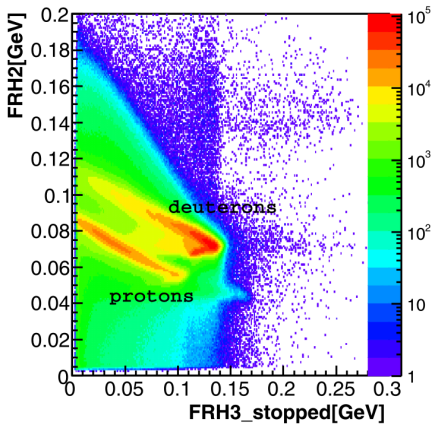

Fig. 2. Example of the ΔE–E identification spectrum collected at 340 MeV beam energy obtained with the use of the Forward Detector.

After the selection of the proton–proton coincidences and having performed the energy calibration, any kinematical configuration of the breakup reaction within the angular acceptance of the detection system can be analysed. The position-sensitive detection system allows to determine polar angles with precision better than 1°. The data were integrated within angular ranges of $\theta_{1,2}$ (±1°) and φ_{12} (±5°). These ranges are larger as compared

to angular resolution of the detectors and, therefore, no significant systematic uncertainty is related to the determination of solid angles obtained for selected configurations. The effect of averaging is taken into account when comparing the data with the theoretical calculations, averaged accordingly. The sample kinematical spectra E_1 *versus* E_2 are shown in Fig. 3. The central line of the experimental band of the registered kinematical spectrum is lying on the theoretical kinematics. It confirms the correct energy calibration. The energy threshold for the identification of protons in the Forward Detector is about 60 MeV. Events belonging to the configuration of interest are projected onto the kinematical curve corresponding to the point-like, central geometry. To determine the contribution of the background, the events were divided into 8 MeV widths slices along S (arclength). Only events concentrated around kinematical curve within the band of D-values ranging from -20 MeV to 20 MeV were taken into account (Fig. 3).

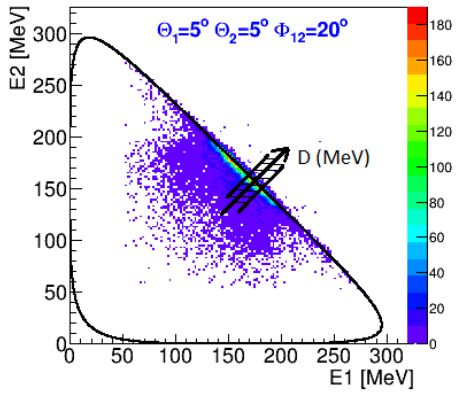

Fig. 3. E_1 *vs.* E_2 coincidence spectrum of the two protons registered at $\theta_1 = 5° \pm 1°$, $\theta_2 = 5° \pm 1°$, and $\varphi_{12} = 20° \pm 5°$. The solid line shows a three-body kinematical curve, calculated for the central values of experimental angular ranges. D axis in the picture denotes the distance of the (E_1, E_2) point from the kinematical curve. Box represents example of integration limits ($\Delta S = 8$ MeV) for a sample S-slice.

Number of events obtained after background subtraction is presented as a function of the arclength S. After normalization to the integrated luminosity and including detector acceptance, all cuts applied in the analysis, detector efficiency, the differential cross section is obtained. To obtain the differential cross section of the breakup reaction with precision relevant to study the 3NF or relativistic effects proper determination of above corrections are very important. All these steps of analysis should be controlled with a high accuracy.

3.1. Detection efficiency

WASA Monte Carlo program was used for the precise determination of efficiency of the detection system. Including detector acceptance and all cuts applied in the analysis, detector efficiency for registering and identifying elastically scattered deuterons is about 80%. The efficiency of the detection system for proton–proton coincidences obtained for each kinematical configuration with defined integration limits: $\Delta\theta_1 = \Delta\theta_2 = 2^\circ$ and $\Delta\varphi_{12} = 10^\circ$ is presented in Fig. 4.

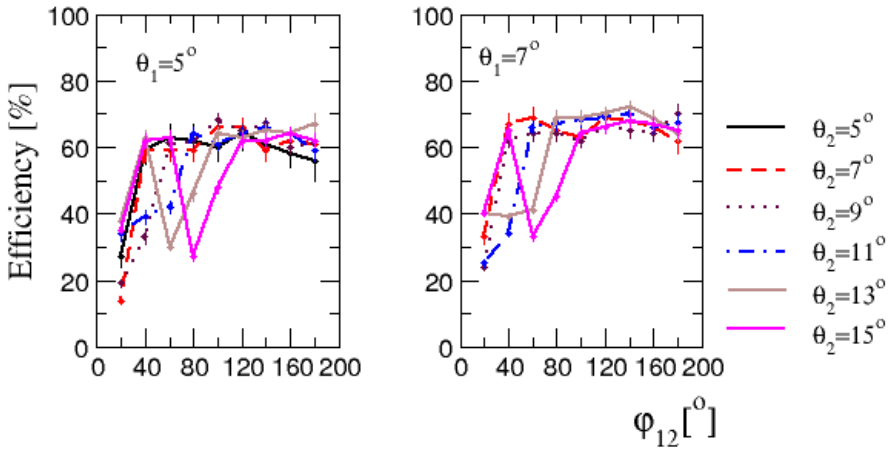

Fig. 4. The efficiency of the detection system for proton–proton coincidences obtained for chosen kinematical configuration (θ_1, θ_2, φ_{12}) using MC simulation.

3.2. Cross-section normalization

For the purpose of normalization of the experimental results, the luminosity is determined on the basis of the number of the elastically-scattered deuterons at a given θ angle, measured in parallel to the breakup reaction, and on the known cross section for elastic scattering at the studied energy [10]. The integrated luminosity is given by the formula

$$L = \frac{N_{\mathrm{el}}(\theta_d)}{\sigma^{\mathrm{el}}_{\mathrm{LAB}}(\theta_d)\Delta\Omega_d\epsilon^{\mathrm{el}}(\theta_d)}\,, \tag{1}$$

where N_{el} is a number of elastically scattered deuterons registered at the deuteron angle θ_d (during the same time period as breakup events) and $\Delta\Omega_d$ ($\Delta\Omega_d = 2\pi\Delta\theta_d \sin\theta_d$) is the solid angle for registering deuterons. $\sigma^{\mathrm{el}}_{\mathrm{LAB}}(\theta_d)$ is the value of elastic scattering cross section, $\epsilon^{\mathrm{el}}(\theta_d)$ is a product of all efficiencies determined on the base of MC simulations.

The values of the luminosity presented as a function of the deuteron scattering polar angle for the sample of data are shown in Fig. 5. The error bars represent statistical uncertainties only. The boxes represent systematic errors due to normalization either to calculated or measured (at 170 MeV, [10]) cross section and/or uncertainty related to the subtraction of the proton background (dominating at $\theta_d = 14°$). Taking into account systematic errors, the results obtained in the range of angles between 9° and 13° are consistent and their average is calculated.

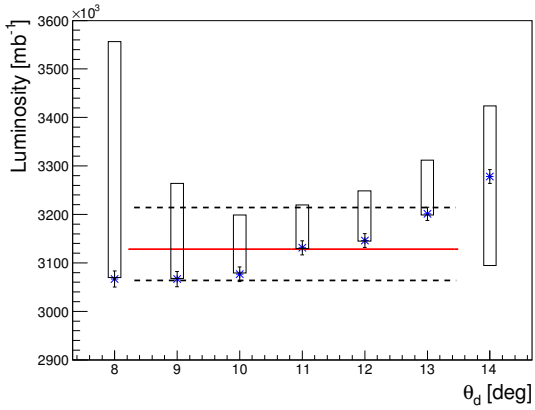

Fig. 5. Determination of the integrated luminosity. Values of the luminosity are presented at several deuteron polar angles, θ_d. The error bars represent statistical uncertainties. The solid line corresponds to the weighted average of five results with the smallest systematic errors (shown as boxes). The dashed lines represent the range of systematic error (2%–3%) taking into account to systematic uncertainties of all experimental points from the range between 9° and 13°.

The differential breakup cross section for a chosen angular configuration normalized to luminosity value (Eq. (1)) is given by the following formula:

$$\frac{\mathrm{d}^5\sigma(S,\Omega_1,\Omega_2)}{\mathrm{d}\Omega_1\mathrm{d}\Omega_2\mathrm{d}S} = \frac{N_{\mathrm{br}}(S,\Omega_1,\Omega_2)}{L\,\Delta\Omega_1\Delta\Omega_2\Delta S\epsilon^{\mathrm{br}}(S,\Omega_1,\Omega_2)}\,, \tag{2}$$

where N_{br} is the number of breakup coincidences registered at the angles Ω_1, Ω_2 and projected onto a ΔS-wide arclength bin. Subscripts 1 and 2 refer to the first and second proton registered in coincidence. $\Omega_i \equiv (\theta_1, \varphi_i)$, with $i = 1, 2$, are the polar and azimuthal angles, respectively, and $\Delta\Omega_i$ is the solid angle ($\Delta\Omega_i = \Delta\theta_i\Delta\varphi_i \sin\theta_i$). $\epsilon^{\mathrm{br}}(S,\Omega_1,\Omega_2)$ contains the product of all relevant efficiencies determined for each angular configuration.

3.3. Experimental uncertainties

Statistical errors of the measured cross-section values comprise an uncertainty of the measured number of the breakup coincidences and of the luminosity. This statistical error per point of the cross-section data in 189 kinematic configurations is below 2% (in maxima of the cross-section distributions).

The systematic error of the cross section stems primarily form uncertainty of determination of efficiency for proton–proton coincidences which varies between 1% and 7%, reaching up to 11% for configurations with the lowest $\varphi_{12} = 20^\circ$ (see Fig. 4). In conclusion, systematic uncertainties vary between 4% and 10%.

3.4. Breakup cross section

Examples of the normalized experimental breakup event rate obtained for the chosen kinematical configurations at the energy of 340 MeV are presented in Fig. 6. In the figures, the error bars represent the statistical uncertainties. The systematic uncertainties are represented by grey/cyan bands in the lower part of each individual panel. The data have been compared to calculations performed by two theory groups (H. Witała *et al.*, A. Deltuva) with the state-of-the-art $2N$ potentials, combined with $3N$F, Coulomb interaction or carried out in a relativistic regime. The result presented in the left panel indicates an interplay of $3N$F effects, Coulomb force and relativistic effects. For the configuration shown in the right panel, the calculations underestimate the experimental data. The discrepancy is even increased by relativistic calculations. Is it due to missing large $3N$F contribution?

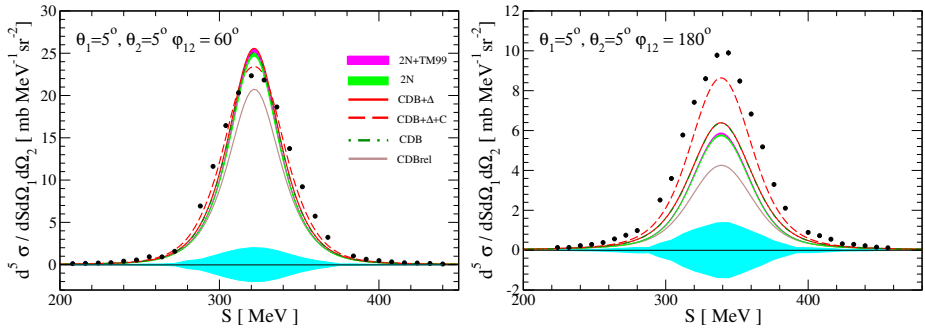

Fig. 6. Examples of the differential cross section of breakup reaction at beam energy of 340 MeV obtained as a function of the S value for chosen kinematic configurations (indicated in the panels). Data (black dots) are compared to results of theoretical calculations designated in the figures. Statistical errors are smaller than the point size. The grey/cyan bands show ranges of systematic uncertainties.

4. Summary and outlook

The analysis is continued with the aim to determine the differential cross sections for the the deuteron breakup process in the $d+p$ system at energies of 380 and 400 MeV, performed for a large set of kinematic configurations covering a significant part of the reaction phase space (for large polar angles). The data will be compared to the theoretical predictions for three nucleon systems. The calculations including relativistic effects with $3N$Fs and studies of the Coulomb effects are very important to draw definitive conclusions.

REFERENCES

[1] W. Glöckle *et al.*, *Phys. Rep.* **274**, 107 (1996).

[2] A. Deltuva, K. Chmielewski, P.U. Sauer, *Phys. Rev. C* **67**, 034001 (2003); A. Deltuva, R. Machleidt, P.U. Sauer, *Phys. Rev. C* **68**, 024005 (2003).

[3] E. Epelbaum, *Prog. Part. Nucl. Phys.* **57**, 645 (2006).

[4] R. Machleidt, F. Samaruca, *Phys. Scr.* **91**, 083007 (2016).

[5] A. Deltuva, A.C. Fonseca, P.U. Sauer, *Phys. Rev. C* **72**, 054004 (2005); **73**, 057001 (2006).

[6] R. Skibiński, H. Witała, J. Golak, *Eur. Phys. J. A* **30**, 369 (2006).

[7] H. Witała *et al.*, *Phys. Rev. C* **83**, 044001 (2011).

[8] Chr. Bargholtz *et al.*, *Nucl. Instrum. Methods Phys. Res. A* **594**, 339 (2008).

[9] H. Adam *et al.*, `arXiv:nucl-ex/0411038`.

[10] K. Ermisch *et al.*, *Phys. Rev. C* **68**, 051001(R) (2003).